Deformations during jet–stripping in the galvanizing process

Article *in* Journal of Engineering Mathematics · July 2011

Impact Factor: 0.8 · DOI: 10.1007/s10665-010-9394-8

4 authors, including:

Graeme Charles Hocking
Murdoch University
76 PUBLICATIONS **746** CITATIONS
SEE PROFILE

Alistair Fitt
Oxford Brookes University
103 PUBLICATIONS **795** CITATIONS
SEE PROFILE

Chris Breward
University of Oxford
42 PUBLICATIONS **604** CITATIONS
SEE PROFILE

Deformations during jet-stripping in the galvanizing process

G.C. Hocking (g.hocking@murdoch.edu.au)
Mathematics & Statistics, Murdoch University, Perth, Australia

W.L. Sweatman (w.sweatman@massey.ac.nz)
Massey University, Auckland, New Zealand

A.D. Fitt (a.d.fitt@soton.ac.uk)
University of Southampton, Southampton, UK

C. Breward (breward@maths.ox.ac.uk)
University of Oxford, Oxford, UK

Abstract. The problem of coating steel by passing it through a molten alloy and then stripping off excess coating using an air jet is considered. The work revisits the analysis of Tuck [1] with the addition of extra shear terms and a consideration of the effect of increased air-jet speeds. A first-order partial differential equation is derived and solved both to obtain the steady-state coating shape and to determine the evolution of any defects that may form.

Keywords: Jet-stripping, viscous flows, coating flows

1. Introduction

During the production of steel strips, it is usual to coat the steel surface with a layer of metallic alloy (e.g. zinc/aluminium) for protection from corrosion. One way in which this can be achieved is to use the "continuous hot-dipped galvanising process" during which the steel strip is passed through a bath of the molten metal coating. After passing through the bath the coated steel strip is pulled upward and the alloy coating cools and solidifies. (The uncoated steel surface is protected from corrosion prior to entering the bath.)

A pair of air knives lie on either side of the ascending steel strip. These control the thickness of the metal coating. Each air knife fires a high velocity air stream along a horizontal line across the rising strip. This forces some of the molten metal to return downwards into the bath, leaving the coating at the desired thickness.

Tuck and other authors [1, 2, 3, 4] built on the work of Thornton and Graff [5] to develop a model for this process that assumed the coating was thin and the flow was almost-uni-directional. The air jet was modelled as a surface pressure distribution. The resulting first-order partial differential equation was analysed in some depth and it was shown that

the coating thickness was dominated by a control point that coincided with the minimum of the maximum upward flux of the coating material. This calculation turned out to be rather delicate and in the actual production process an iterative scheme is used. Tuck [1] also showed that small perturbations in the surface shape were marginally stable. Subsequent work has shown that the air shear due to the air knife is important, as can be verified by a dimensional analysis. This extra term in the equation makes the problem more complicated, but does not change the essential features.

During recent developments in the production process, problems have arisen with the quality of surface coatings. These have involved some new advanced alloy coatings. With fixed processing conditions (speed of the strip, alloy used, etc.), there is an associated air knife pressure below which satisfactory coating takes place but above which coating defects may appear. The defects take various forms. These include waves, lines and pocks. Of these the pocks are the most serious as they correspond to a substantial local thinning of the coating which will produce a dramatic reduction of the corrosion protection.

An improved model has been developed. Steady-state conditions are found and then several different perturbations are considered to investigate whether increased pressure causes possible instabilities in the flow. Simulations are carried out to further explore the problem and to verify the theoretical conclusions.

2. Modelling the coating process

The development of the mathematical model (also described in [6]) parallels that of Tuck [1]. The resulting equations are the same but with the addition of a term for the surface shear stress due to the air knife. We adopt the coordinate scheme shown in Figure 1. The flow is assumed to be two-dimensional, incompressible, laminar and unsteady.

The flow is governed by the two-dimensional Navier-Stokes equations

$$u_t + uu_x + wu_z = -\frac{1}{\rho}p_x + \frac{\mu}{\rho}(u_{xx} + u_{zz}) - g \tag{1}$$

$$w_t + uw_x + ww_z = -\frac{1}{\rho}p_z + \frac{\mu}{\rho}(w_{xx} + w_{zz}) \tag{2}$$

$$u_x + w_z = 0 \tag{3}$$

where t denotes time, x and z respectively denote the vertical and horizontal coordinates, $\vec{q} = (u, w)$ denotes the fluid velocity, p denotes pressure, ρ denotes density, μ denotes dynamic viscosity, and g is the

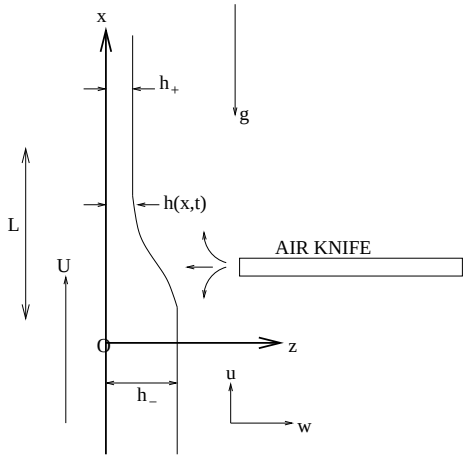

Figure 1. A schematic of the coordinate system and nomenclature

acceleration due to gravity. Subscripts are used to indicate differentiation. In addition to the initial condition that is required to specify the problem, there are boundary conditions

$$u = U, \quad w = 0 \quad \text{at} \;\; z = 0 \tag{4}$$

$$\mu u_z = \tau_a(x), \quad p - p_a(x) = -\gamma\kappa, \quad h_t + uh_x = w \;\; \text{at} \;\; z = h(x,t), \tag{5}$$

for which U denotes the speed of the coating substrate, $z = h(x,t)$ is the equation of the coating layer's free surface, γ is surface tension and κ is curvature. The pressure $p_a(x)$ and the shear stress $\tau_a(x)$, that are applied by the action of the air knife, are both assumed to be specified. As the rate of change of h with x is small, the curvature $\kappa \approx h_{xx}$.

The equations (1)-(3) and boundary conditions (4)-(5) are non-dimensionalised as follows. We set $x = L\bar{x}$, $z = \epsilon L\bar{z}$, $u = U\bar{u}$, $w = \epsilon U\bar{w}$, $t = (L/U)\bar{t}$, $p = (\mu U/\epsilon^2 L)\bar{p}$, $h = \epsilon L\bar{h}$, $\tau_a(x) = (\mu U/\epsilon L)G(x)$ and $p_a(x) = (\mu U/\epsilon^2 L)P(x)$. Here bars denote non-dimensional variables, L denotes a typical length over which the air knife is active, and $\epsilon = h_0/L << 1$ where h_0 is a typical value of h. With these scalings, dropping the overbars for convenience, the equations and boundary conditions become, to leading order,

$$p_x = u_{zz} - S, \quad p_z = 0, \quad u_x + w_z = 0 \tag{6}$$

$$u = 1, \quad w = 0 \quad \text{at} \;\; z = 0 \tag{7}$$

$$u_z = G(x), \quad p - P(x) = -Ch_{xx}, \quad h_t + uh_x = w \quad \text{at} \;\; z = h, \tag{8}$$

where S is the Stokes number and C is the product of ϵ^3 with the inverse of the Capillary number $Ca = \mu U/\gamma$,

$$S = \frac{\epsilon^2 \rho g L^2}{\mu U} \quad \text{and} \quad C = \frac{\epsilon^3 \gamma}{\mu U}.$$

$P(x)$ and $G(x)$ are nondimensional air pressure and shear acting on the surface of the coating. Terms multiplied by $\epsilon^2 Re = h_0^2 \rho U/(\mu L) \approx 0.03$ (see values in Appendix 1) have been ignored in accordance with the usual "thin layer" assumptions. The magnitude of the inertial terms is not as small as one would like, but the effectiveness of the approximation is clear from comparisons with the application in the industrial setting. Solving (6)-(8), we find that

$$p = P(x) - Ch_{xx} \tag{9}$$

$$u = (S + P'(x) - Ch_{xxx}) \left(\frac{1}{2} z^2 - hz \right) + zG(x) + 1 \tag{10}$$

$$w = -(P''(x) - Ch_{xxxx}) \left(\frac{1}{6} z^3 - \frac{1}{2} hz^2 \right) + \tag{11}$$

$$\frac{1}{2} z^2 h_x (S + P'(x) - Ch_{xxx}) - \frac{1}{2} z^2 G'(x). \tag{12}$$

The pressure and velocity components in (9)-(12) now satisfy all of the equations and boundary conditions (6)-(8) apart from the last boundary condition. This final condition now gives a PDE governing the evolution of $h(x,t)$,

$$h_t + \left(h + \frac{1}{2} h^2 G(x) - \frac{1}{3} h^3 (S + P'(x) - Ch_{xxx}) \right)_x = 0. \tag{13}$$

Henceforth, surface tension will be neglected since $C \approx 2.5 \times 10^{-6}$ suggests this term plays no significant role. A consideration of this factor can be found in Tuck et al [3]. Before we begin to examine the behaviour of waves or pock-marks, we need to consider the matter of steady-state solutions to (13).

3. Steady state solutions

The steady state equation is obtained by omitting the time dependent term from (13). The surface coating thickness $h(x)$ is then a function of x only, leaving

$$Q = f(h,x) = h + \frac{h^2}{2} G(x) - \frac{h^3}{3} (S + P'(x)), \tag{14}$$

where Q is a constant that must be the flux of fluid in the coating layer. The flux Q must remain constant as x varies. However, the coefficients of the cubic expression, equation (14), will vary continuously with changes in the shear stress and pressure ($G(x)$ and $P(x)$). The steady solution is therefore determined by obtaining the value of the constant, Q for a given $P(x)$ and $G(x)$.

In [1, 6], it was shown that this cubic equation can be used to obtain the control point, $h = h_c$ that determines the value of Q_c by finding the point at which the cubic has a double root. Tuck [1] showed that this point corresponded to the minimum of the maximum possible fluxes at each section (and gave a nice explanation as to why this might be so).

Noting that if we are at the control point (x_c, h_c), then

$$\frac{\partial f}{\partial h}(h_c, x_c) = 1 + h_c G(x_c) - h_c^2[S + P'(x_c)] = 0, \tag{15}$$

and so h_c satisfies

$$h_c = \frac{1}{2}\left[\frac{G(x_c)}{S + P'(x_c)}\right]\left(1 \pm \sqrt{1 + 4\left[\frac{S + P'(x_c)}{G(x_c)^2}\right]}\right). \tag{16}$$

It is possible to show that the negative sign is appropriate here.

The flux Q must be identical for all values of x and from (14), we find

$$\frac{dQ}{dx} = 0 = h'[1 + hG(x) - h^2(S + P'(x))] + \frac{h^2}{2}G'(x) - \frac{h^3}{3}P''(x).$$

Evaluating this at $x = x_c$, using (15) and the fact $h_c \neq 0$, we obtain

$$G'(x_c) = \frac{2}{3}h_c P''(x_c). \tag{17}$$

Possible locations of x_c and values of h_c are therefore determined by solutions to (15) and (17), whence the flux Q_c that is required is given by $Q_c = f(h_c, x_c)$.

A simple implementation of this is to evaluate h_c at each point x from (16) and then find the corresponding flux Q^* at each point from (14). The correct values of x_c and h_c are then those corresponding to the minimum, Q_c^*.

Implementing this algorithm provides a typical steady-state solution, as shown in Figure 2. In [6] some functions were chosen to replicate the behaviour of the pressure and shear, but they were only qualitatively correct. Here, we use for the Stokes number and pressure

$$S = 0.0015, \quad P(x) = P_{\mathrm{MAX}}(1 + 0.6x^4)^{-3/2} \tag{18}$$

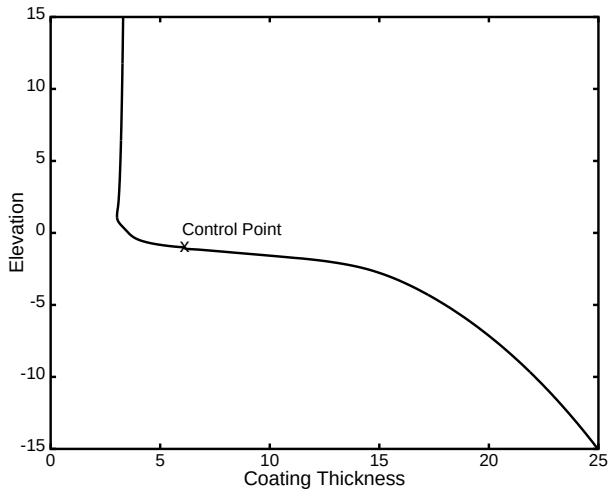

Figure 2. Typical steady-state solution $S = 0.0015,\ P_{\mathrm{MAX}} = 0.01,\ G_{\mathrm{MAX}} = 0.1$. The control point of the flow is indicated.

and for the shear,

$$G(x) = \begin{cases} \mathrm{sgn}(x) G_{\mathrm{MAX}} \left[\mathrm{erf}(0.41|x|) + 0.54|x| e^{-0.22|x|^3} \right], & \text{if } |x| < 1.73, \\ \mathrm{sgn}(x) G_{\mathrm{MAX}} \left[1.115 - 0.25 \log |x| \right], & \text{if } |x| \geq 1.73. \end{cases} \tag{19}$$

These functions were taken from the experimental work of Tu et al [8] and Elsaadawy [9]. In Figure 2, using $P_{\mathrm{MAX}} = 0.01$, $G_{\mathrm{MAX}} = 0.1$ gives $x_c \approx -1.107$, $h_c \approx 6.172$, the flux is given by $Q_c \approx 3.529$, the upstream coating thickness is given by $h_- \approx 43$ and the downstream thickness by $h_+ \approx 3.33$.

The effect of the pressure and shear distribution on the downstream thickness can be seen in Figure 3. This figure is equivalent to Figure 5 of Tuck [1]. Clearly the final coating thickness decreases as the pressure of the air jet increases. Corresponding to this is a growth in thickness of the upstream layer as more of the coating material drains downward. The optimal flux decreases as the coating thickness is reduced, as would be expected. The result of Thornton and Graff [5] that the final coating thickness (shown as the solid line in Figure 3) is approximated well by the value of the optimal flux (dashed line) as the pressure increases is clearly seen.

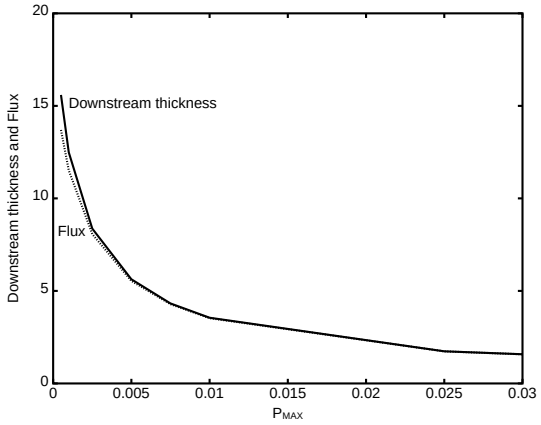

Figure 3. The effect of changing pressure and shear stress on the downstream coating thickness and flux. The dashed line is the flux. These become more alike as $P_{\rm MAX}$ increases. In all cases $G_{\rm MAX} = 10P_{\rm MAX}$

4. Analysis of the unsteady equation

Consider a coating process that is established and running in steady state. As x increases from h_- to h_+, the coating varies smoothly under the action of the air knife as described in Section 3. Thus $h = h^\circ(x)$ where h° is determined by

$$h^\circ + \frac{(h^\circ)^2}{2}G(x) - \frac{(h^\circ)^3}{3}(S + P'(x)) = Q_c$$

and Q_c by solutions to (15) and (17). In [6] an analysis was performed on the fate of small disturbances to the steady solution. In short, this suggested that there were regions in which it was possible for disturbances to grow in amplitude if a number of conditions were met. Using the pressure and shear distributions approximating realistic functions it is possible to consider this behaviour more carefully. If we re-write equation (13) in the form

$$h_t + c(h, x)h_x = A(h, x), \tag{20}$$

we can see that

$$c(h, x) = 1 + G(x)h - h^2(S + P'(x)) \tag{21}$$

represents the speed at which a disturbance will propagate and

$$A(h, x) = h^2(hP''(x)/3 - G'(x)/2) \tag{22}$$

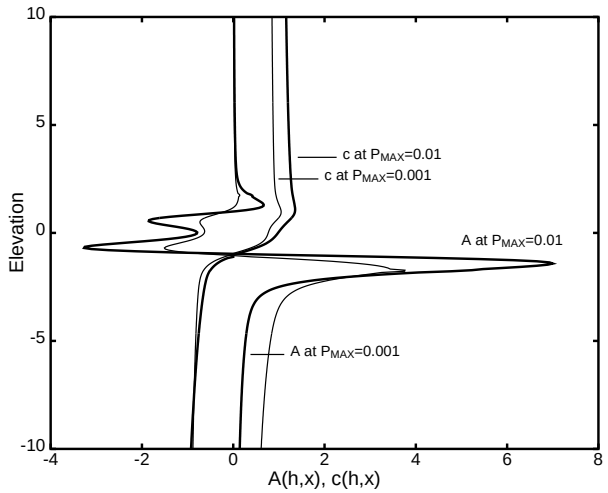

Figure 4. Terms $c(h,x)$ and $A(h,x)$ as a function of elevation x for the steady solution for cases $P_{\rm MAX} = 0.001, 0.01$ (thicker lines)

represents growth or decay of the signal. If we plot these we can estimate what will happen. Tuck [1] found that (given his equations (22,23)) the value of $c(h,x)$ was less than zero if $x < x_c$ and greater than zero if $x > x_c$ and it is trivial to show this to be true here also; note that $c(h,x) = 0$ at (x_c, h_c) from (15). This means that disturbances created before the control point will propagate downwards, back toward the bath, while those formed after the control point will propagate upwards and are of major interest.

Figure 4 shows typical forms for $c(h,x)$ and $A(h,x)$ along the length of the region for a weaker jet, $P_{\rm MAX} = 0.001$, and a stronger one, $P_{\rm MAX} = 0.01$. It verifies the results of the linear analysis [1, 6], but also shows that the term $A(h,x)$ is only significant over a very narrow region close to the control point, whereas the wave speed term $c(h,x)$ remains significant well downstream where it approaches $1 - h^2 S$. Further, for the weaker jet, gravity plays a more significant role as h is larger and $G(x)$ is smaller.

The fact that $A(h,x)$ remains small for all pressures suggests that outside of the region of influence of the jet, a disturbance will be marginally stable (neither growing nor decaying) confirming the analysis of Tuck [1].

Hocking et al [6] showed that using different functional forms for the shear and pressure terms different types of breaking behaviour could be set up. Here we choose to consider only the more realistic forms (18,19).

Close to the centre line of the jet the behaviour is dictated by the presence of the jet and the interaction between the shear and pressure terms. There are regions where higher points travel faster and others where they travel more slowly, see [6]. Outside of this narrow region, $c(h,x) \approx 1 + G(x)h - h^2S$. In the higher pressure case, the value of $c(h,x)$ is affected much more profoundly by the shear term. If $c(h,x) > 1$ (the high pressure case), then disturbances will travel upward faster than the substrate is travelling, and depressions will break forward (upward). If $c(x,h) < 1$ (lower air jet pressure) disturbances travel more slowly than the sheet and depressions will break backward (downward) into themselves. In the case of bumps, the breaking should be in the opposite direction.

To test these conclusions, we performed numerical studies to examine different scenarios.

5. Numerical studies

An accurate numerical scheme was developed using the method of lines. This method is described in detail in [10], which also provides finite difference formulae that are of fourth-order (or higher) accuracy for the spatial derivatives. Given a set of values for $h(x,t)$ at any time at a discrete set of x values in equation (20) with (21) and (22), and inputing the known values of $P(x), G(x)$ and S and their derivatives, an expression for h_t can be computed at each point using the fourth-order formulae of [10]. These were then integrated forward in time using *Octave's* fourth-order *lsode* routine from an initial state $h(x,0) = h^\circ$ with some perturbation (if necessary) as described below.

The characteristics method used in [6] was very accurate, but could not be used when the pressure of the jet was varied with time because of the tendency of points below the control point to move downward and those above to move upward, leaving minimal resolution near the central region. The solutions using the method of lines were compared with those of the very accurate method of characteristics [6] and found to agree to graphical accuracy for all cases. The method used does not have the capability to capture shocks, but we are not interested in following shocks or the actual breaking of wave disturbances other than to determine if and when they occur.

In all of the simulations that are described below, the initial condition was chosen as the appropriate steady solution computed as described above. Cases were considered by either placing an indentation or bump in the steady solution, to compute the evolution of such under

different conditions, or the pressure was pulsed to simulate a "shudder" in the air-knife.

5.1. Results - Spatial Disturbance

A dip of the form $\delta(x) = -0.3e^{-(x-0.5)^2}$ was added to the steady state coating thickness with "experimental" values $S = 0.0015$ and a range of values $P_{\rm MAX} = 0.005, 0.05, 0.01$ and 0.05 with $G_{\rm MAX} = 10P$MAX and its evolution was followed as it travelled upward. The results of these simulations are shown in Figure 5, in which the same dip is shown at different times separated by three non-dimensional time units. The different speeds at which the outer edge of the coating and hence the disturbance moves can clearly be seen, as the sheet is moving at the same speed in each case. Note that as the disturbance passes the coating returns to the "steady" position.

At lower values of $P_{\rm MAX}$, it is clear that the region that is influenced by the air jet is very narrow and so the flow is quickly dominated by the shear and gravity, meaning that points further from the substrate travel more slowly. Therefore, the indentation steepens at the leading edge as a prelude to breaking backward into itself.

At the highest values of $P_{\rm MAX}$, when the coating is very thin, the shear terms continue to play a role for some time, and create a situation in which the points deeper in the depression move more slowly, thus leading to the back of the indentation breaking forward into the hole.

The behaviour for the two intermediate values of $P_{\rm MAX} = 0.01, 0.005$ in Fig. 5 show that the depression persists for a long distance up the sheet with only minor perturbations to its shape.

The behaviour of a bump rather than a depression was also as expected, with bumps breaking backward at lower pressures and forward for higher values, consistent with the comments above. Again, there is a middle region where the bumps will persist.

If the coating is thick, as for $P_{\rm MAX} = 0.0025$, the speed c depends on h^2 and is large enough for the breaking to occur reasonably quickly. If h is very small, then not only is the coating disturbance moving upward more quickly, the effect of gravity is greatly diminished, so that a disturbance will remain almost unchanged for a significant distance (see Figure 5).

5.2. Results - Pressure variation

Further simulations were conducted in which the pressure of the air knife was varied with time. In the first case a single pulse in which the pressure momentarily dropped by a maximum of 20% (and then

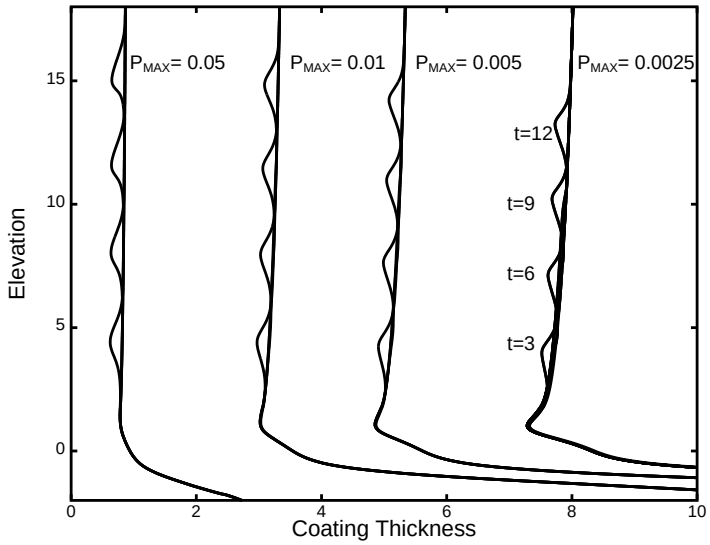

Figure 5. Evolution of a single depression separated by $\Delta t = 3$ time units for cases of different applied pressures of the air knife. In each case, $G_{\mathrm{MAX}} = 10P_{\mathrm{MAX}}$. The unperturbed line is the steady coating shape in each case.

returned to the original value) was considered and in the second case it was varied sinusoidally.

The results of the single pulse for the case of $P_{\mathrm{MAX}} = 0.01$ are shown in Figure 6. They show that even with such a large pulse only a small dip is created. The pulse generates fairly long wave disturbances that can be seen propagating both upward and downward. The downward travelling bump steepens quite rapidly due to the thickness of the layer there. Once created, the upward travel of the dip follows the pattern of the dips considered in the previous section.

In the second simulation, the pressure was pulsed according to $P(x)+\delta_P(x,t) = P(x) + D_P \sin \omega t$, where D_P represents the amplitude of the "shudder". Results of these simulations are not shown because the disturbance to the steady state appeared to be minimal, even with D_P as large as 0.2, i.e. a 20% variation in amplitude. A range of different frequencies were tried at the higher end of the spectrum with similar minimal effect. Low frequency variations would not be shudder and would be expected to behave like the single pulse case.

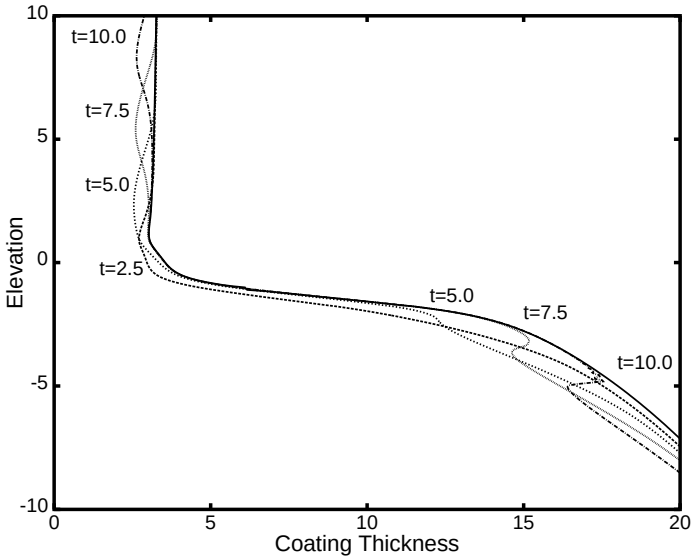

Figure 6. Development of a depression caused by a single pressure drop. Here, $P_{\mathrm{MAX}} = 0.01, G_{\mathrm{MAX}} = 0.1$. The dip, once initiated, behaves in a similar manner to those considered above while the remaining surface quickly returns to the steady solution. The wiggles in $t = 10$ at the bottom are caused by numerical error as a shock forms.

6. Conclusions

We have modified the equations derived by Tuck [1] to include a shear term as in [6] and adapted the analysis accordingly. In addition, we have used empirically determined shape functions ([4, 7, 8, 9]) for the pressure and shear.

The results suggest that what happens to a disturbance, once created, depends on the shear generated by the air jet at higher values and is dominated by gravitational effects at lower values. Numerical results confirm this hypothesis. However, there is no doubt that disturbances of any sort will persist much further up the sheet if the coating is thinner, as the effect of gravity on the thinner coatings is not sufficient to cause the dip to break back into itself and close. Surface tension and metallurgical effects of solidification may combine to reduce the size of these disturbances or prevent breaking of the waves in some cases. However, surface tension is likely to play a very small role except in exceptional circumstances [3]. Metallurgical effects are beyond the scope of the present analysis and will occur beyond the region of interest considered here.

It is of some interest to examine the dimensional values, although they are dependent on the choices for the "typical" values and occur in quite complicated combinations. However, using the values given in Appendix A, $P_{\mathrm{MAX}} \approx 0.01$ (for which the air jet speed is $28ms^{-1}$ and the sheet is moving up at $2.5\ ms^{-1}$) corresponds to a final coating thickness of around $15\mu m$. Effectively higher P_{MAX} values can be obtained by increasing the air jet speed or decreasing the speed of the sheet. If we take this to be a typical case, the transition to potential "problem" cases would occur when the coating thickness drops below $h \approx\ 1$ (a "real" value of around $5\ \mu m$) which corresponds to $P_{\mathrm{MAX}} \approx\ 0.05$ or a doubling of the air-jet speed (see Figure 5) in combination with a slowing of the upward speed of the sheet. It is clear that a significant increase in air jet speed is required to obtain thinner coats unless the upward speed of the sheeting is reduced. Slowing the sheet speed, although it has the apparent effect of an increase in pressure, does allow more time for any dips or bumps to "break" or even out. The accuracy of these calculations in a real situation depends on the actual values for the other parameters and these numbers are given as an indication only.

The work of Tuck [1] has been largely validated as a basis for considering this problem. His conclusion of any disturbance being marginally stable is accurate and it is the fact that the propagation speed depends on the coating thickness that provides some clue as to why a thinner coating may lead to problems.

Importantly, there is no evidence of any "catastrophic" change in the fluid dynamics of the process at higher air jet pressures that might be responsible for the pitting of the surface, but it is clear that any damage to the surface coating is more likely to persist if the coating is thinner.

Appendix

A. Typical values used;

The list below gives typical values used in this work.

- d = half-width of the steel strip $\approx 10^{-3}$m
- g = gravitational acceleration ≈ 9.8 m s^{-2}
- γ_0 = surface tension coefficient of the coating layer $\approx 10^{-1}$ N m^{-1}
- h_0 = scale of thickness of coating layer $\approx 5 \times 10^{-6}$ m
- L = vertical length scale - half-width of air jet $\approx 5 \times 10^{-3}$m
- μ = dynamic viscosity of the coating $\approx 10^{-3}$ kg m^{-1}s^{-1}
- ρ = density of the coating $\approx 3 \times 10^3$ kg m^{-3}
- ρ_s = density of steel $\approx 7 \times 10^3$ kg m^{-3}
- U = upward speed of the metal sheet ≈ 2.5 m s^{-1}
- U_a = maximum centerline speed of the air jet ≈ 30 m s^{-1}

Using these values, the scalings for the pressure and shear stress are

- Pressure scaling $\frac{\mu U}{\epsilon^2 L} \approx 5 \times 10^5$ kg m^{-1}s^{-2}
- Shear scaling $\frac{\mu U}{\epsilon L} \approx 500$ kg m^{-1}s^{-2}

and the non-dimensional quantities that appear are

- Capillary number (Surface tension) Ca= $\frac{\mu U}{\gamma_0} \approx 2.5 \times 10^{-2}$
- Reynolds number Re = $\frac{\rho U L}{\mu} \approx 33,750$
- Stokes number $S = \frac{\rho g h_0^2}{\mu U} \approx 0.0002$
- Length ratio $\epsilon \approx 10^{-3}$

Acknowledgements

We are grateful to Cat Tu and Daniel Yuen from Bluescope Steel, Wollongong, Australia for their discussion and input.

References

1. Tuck EO (1983) Continuous coating with gravity and jet stripping. Phys. Fluids, **26**, (9), pp.2352-2358.
2. Tuck EO, Bentwich M & Van der Hoek J (1983) The free-boundary problem for gravity-driven uni-directional viscous flows. *IMA J. Applied Maths*, 30, 191-208.
3. Tuck EO & Vanden-Broeck J-M (1984) Influence of surface tension on jet-stripped continuous coating of sheet materials. *Amer. Inst. of Chem. Engineers J.*, 30, 808-811.
4. Tu CV (1990) Optimisation of lip gap for thin film coating in the jet stripping process. *Proc. 5th Int. Conf. Manufacturing Engineering*, University of Wollongong, Australia.
5. Thornton JA & Graff HF (1976) An analytical description of the jet-finishing process for hot-dip metallic coatings on strip. *Metallurgical & Materials Trans. B*, **7B**, pp.607-618.
6. Hocking GC, Sweatman WL, Roberts ME & Fitt AD (2010) Coating Deformations in the continuous hot-dipped galvanizing process. *Proc. 2009 Mathematics-in-Industry Study Group*, ed. T. Marchant, M. Edwards, G. Mercer, Wollongong, Aust., $ISBN: 978-1-74128-181-1$, pp. 75-89
7. Tu CV, Wood DH & Hooper JD (1994) Small distance impingement of a plane jet, International Colloquium on Jets, Wakes and Shear Layers, Melbourne, Australia, 18-20 April 1994.
8. Tu CV & Wood DH (1996) Wall Pressure and Shear Stress Measurements Beneath an impinging jet. *Experimental Thermal and Fluid Science,* 13:364–373
9. Elsaadawy EA, Hanumanth GS, Balthazaar AKS, McDermid JR, Hrymak AN & Forbes JF (2007) Coating weight model for the continuous hot-dip galvanizing process. *Metallurgical & Materials Trans. B*, **38B**, pp.413-424.
10. Hamdi S, Schiesser WE & Griffiths GW (2007) Method of Lines, *Scholarpedia, 2(7):2859* `doi: 10.4249/scholarpedia.2859`